VERSITA

Synthesis of nanocrystalline nickel and iron carbides by decomposition of hydrocarbons[*]

M. Podsiadły, I. Pełech, U. Narkiewicz[†]

Institute of Chemical and Environment Engineering, West Pomeranian University of Technology,
Pulaskiego 10, 70-322 Szczecin, Poland

Decomposition of hydrocarbons was carried out on nickel and iron catalysts containing small amounts of calcium and aluminum oxides as structural promoters. Decomposition of methane, ethane and ethylene was studied under atmospheric pressure in the temperature range from 500 to 700 °C. The phase composition of the obtained samples was investigated using X-ray diffraction method. The role of nickel and iron carbides in the formation of carbon deposit was discussed.

Keywords: *nanocrystalline nickel carbide; nanocrystalline iron carbide; decomposition of hydrocarbons*

1. Introduction

Recently, many researchers have studied the formation of carbon nanotubes, most often synthesized using the chemical vapor deposition (CVD) method. These processes are catalyzed by transition metals such as nickel, iron or cobalt. The influence of the type of catalyst used on the carbon yield and carbon morphology has been discussed in a number of papers [1–4]. There is no unanimity among researchers as to which metals are the most active in the formation of carbon nanotubes (CNTs). These differences of opinion result from the influence of other parameters (temperature, reaction time, addition of hydrogen or argon to the reaction mixture) on the quantity and quality of carbon [5–7].

Under experimental conditions in which CVD processes are conducted, iron and nickel can be converted into the corresponding carbides. Their role and activity in the process of nanocarbon formation was studied. Several authors claimed that iron carbide in the form of cementite decomposes and is responsible for carbon deposition and the formation of fibrous structures. Deck and Vecchio [8] studied the growth of carbon nanotubes using a wide variety of transition metals as catalysts (Fe, Co, Ni, Cr, Mn, Zn, Cd, Ti, Zr, La, Cu, V and Gd) and benzene as a carbon source. The nanotubes were grown from a compound containing Fe, Co or Ni. Unsuccessful catalysts were found to either have negligible carbon solubility or to form stable carbides. Emmenegger *et al.* [9] investigated the growth of CNTs by acetylene decomposition over a rough film of Fe_2O_3 on an aluminum surface, which transformed into Fe_2O_3, FeO and Fe_3C following the introduction of C_2H_2. After 20 to 30 minutes, the iron carbide started to decompose into Fe and graphite, a process which coincided with the onset of the growth of CNTs. Buyanov *et al.* [10–12] considered the structure of filamentous carbon formed upon the catalytic decomposition of hydrocarbons on iron-group metals and their alloys. They also proposed the so-called "carbide cycle", in which metastable cementite is formed by hydrocarbon decomposition on the free surface of a catalytic particle and decomposed to form graphitized carbon in the proximity of the graphite-covered surface. The equilibrium is reached when the graphite covers a certain part of the surface of a particle. Therefore, the carbide concentration gradient is the driving force behind the carbon diffusion through iron-carbide particles. Ermakova [13] took the "carbide cycle" into account in her mechanism of growth of carbon filaments on iron-carbide particles.

According to Bokhonov and Korchain [14] the "carbide cycle" can also be applied in the case of graphite formation on nickel particles. In contrast to this, Hernadi *et al.* [15, 16] claimed that cementite alone is inactive in the process of synthesis of carbon nanotubes, when using acetylene as a carbon source. However, Vieira *et al.* [17, 18] and Otsuka *et al.* [19] stated that both cementite and iron remain active in the process of hydrocarbon decomposition. The former [17, 18] investigated ethane decomposition on Fe/Al_2O_3 catalyst. The latter [19] studied the activity of Fe_2O_3/Al_2O_3 and Fe_2O_3/SiO_2 in the process of methane decomposition.

In our previous works, we presented the morphology of the obtained materials using iron or nickel as catalyst and hydrocarbons as a carbon source. In general, the catalysts used for the preparation of carbon nanotubes are supported on, *i.a.*, Al_2O_3, ZnO, MgO, SiO_2 and zeolites. However, in this work, we also applied unsupported iron and nickel. In this work, we present the conditions for the creation of nanocrystalline iron and nickel carbides and their influence on the yield of the nanocarbon material obtained during the CVD.

2. Experimental details

Metal carbides were obtained through hydrocarbon decomposition on iron and nickel catalysts. These catalysts were prepared from nickel (II) and iron (III) nitrates with the addition of a small amount of calcium and aluminum nitrates. The salts were dissolved in water and 20 % NH_4OH was added as a precipitating agent to obtain a pH of 8. Metal hydroxides were precipitated from the solution and the deposit was washed with water, filtered and dried at 75 °C. Subsequent calcination was performed at 500 °C for 1 h to obtain precursors of nanocrystalline metals, *i.e.* nickel and iron oxides with a small amount of structural promoters: CaO and Al_2O_3. The total content of these structural promoters did not exceed 3.0 wt.% and their function was to protect fine metal particles against sintering at elevated temperatures. In the final stage of preparation, the precursors of nanocrystalline metals were reduced polythermally at a temperature range from 20 °C to 500 °C for nickel oxides, and from 20 °C
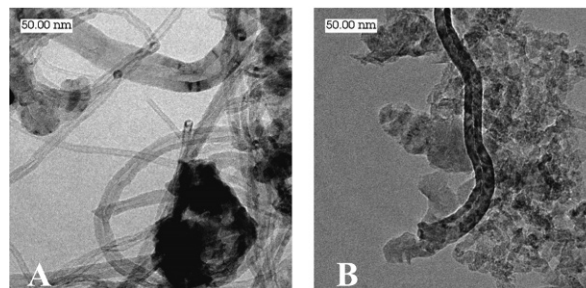

Fig. 1. TEM images of the material obtained by ethylene decomposition on (A) iron- and (B) nickel catalyst.

to 600 °C for iron oxide in a hydrogen atmosphere. After reduction, the samples were cooled to room temperature under nitrogen containing traces of oxygen, to create a very thin passivation oxide layer on the metal surface.

Hydrocarbon decomposition was carried out in a high-temperature furnace (HST 12/400 Carbolite). The samples of the catalyst were placed in ceramic boats inside the quartz tube (diameter 70 mm, length 120 mm). Methane, ethane and ethylene were used as a carbon source. The processes were performed under atmospheric pressure in a temperature range from 500 °C to 700 °C for 1 h. After synthesis, the samples were cooled to room temperature under argon flow.

The phase composition of the obtained catalysts was determined using the X-ray diffraction (XRD) method (Philips XPert).

3. Results and discussion

Nickel and iron catalysts were obtained through co-precipitation of metal precursors with structural promoters. Calcination of the obtained metal hydroxides leads to the transformation of nickel and iron hydroxides into the corresponding oxides. According to XRD analysis (the results of which are not shown here), the samples contain only oxide phases of NiO and Fe_2O_3. In the final stage of synthesis of the catalysts, the transition-metal oxides were reduced to iron and nickel in a hydrogen atmosphere. In order to avoid rapid oxidation of metallic iron and nickel, the samples were then passivated under nitrogen containing traces of oxygen. As a re-

Table 1. The degrees of carburisation on nickel [gC/gNi] and iron [gC/gFe] catalysts obtained in the processes using methane, ethane and ethylene.

carbon source	nickel catalyst			iron catalyst		
	500 °C	600 °C	700 °C	500 °C	600 °C	700 °C
methane	0.15	0.49	0.21	0.18	0.83	2.76
ethane	1.43	2.61	1.75	0.21	0.92	3.99
ethylene	5.69	4.37	10.24	1.15	2.73	12.87

sult, a very thin oxide layer was formed on the metal surface. Detailed investigation of the preparation of catalysts was described earlier.

Hydrocarbon decomposition was carried out in a high-temperature furnace. The morphology of the samples obtained on iron and nickel catalyst after ethylene decomposition at 700 °C was investigated, and TEM images are presented in Fig. 1, panels A and B, respectively. In the case of the sample obtained using iron catalyst, multiwalled carbon nanotubes with diameters ranging from 5 nm to 40 nm were observed. The material obtained using nickel catalyst was more disordered. Thick carbon fibers and fishbone-shaped carbon nanotubes with diameters ranging from 20 nm to 30 nm were observed.

The degree of carburisation of particular samples is presented in Table 1. As a result of the decomposition of methane and ethane on nickel catalyst, the carbon yield increased with an increase in temperature. The maximum carbon yield was obtained at 600 °C. After this point, the carbon yield decreased. In the case of ethylene decomposition, an increase in temperature from 500 °C to 700 °C triggered an increase in the degree of carburisation.

For iron catalyst, higher temperatures led to a higher degree of carburisation, regardless of the kind of carbon source.

The diffraction patterns of nickel catalyst after the decomposition of methane at 500 °C (1), 700 °C (2); ethane at 500 °C (3), 650 °C (4), 700 °C (5); ethylene at 500 °C (6), 600 °C (7), 700 °C (8) are shown in Fig. 2. The phase composition of the samples depended on temperature and the carbon source. After the decomposition of methane (1, 2), low intensity peaks attributed to the graphite phase and to the regular structure of nickel were detected in the samples. Additionally, a small amount of nickel ox-

ide could be observed in the sample. As a result of methane decomposition, a low degree of carburisation, in the range of 0.15 gC/gNi to 0.49 gC/gNi (see Table 1) was achieved. Therefore, the nickel crystallites were not sufficiently covered with a carbon coating and the oxidation reaction could proceed. The samples obtained by ethane decomposition at 500 °C (3) and 600 °C (the diffraction pattern is not shown here) had the same phase composition as the samples obtained by methane decomposition, except the intensity of the graphite peak which was slightly higher as a consequence of higher degree of carburisation. The samples obtained in an ethane atmosphere at 650 °C (4) and 700 °C (5) had a different phase composition. At 650 °C and 700 °C, the nickel carbide phase was observed. However, at higher temperatures, the intensity of the peaks ascribed to Ni_3C was lower. A similar phenomenon was observed for the samples obtained using ethylene as a carbon source. At 500 °C (6), almost all the nickel reacted to nickel carbide and the peaks derived from the nickel phase had a very low intensity. With an increase in temperature to 600 °C (7), the intensity of the nickel carbide peaks decreased, whereas the intensity of the nickel peaks increased. In the sample obtained at 700 °C (8), only a small amount of nickel carbide was observed. In the diffraction patterns (6, 7, 8), the peaks that originated from the nickel oxides were undetectable by XRD method. However, in this case, we cannot exclude the possibility of simultaneous formation of a passive layer of nickel oxide, since the XRD method is not sufficiently sensitive to detect a small amount of this phase.

Taking these results into consideration, we can conclude that both the temperature and the carbon source have a significant influence on the phase
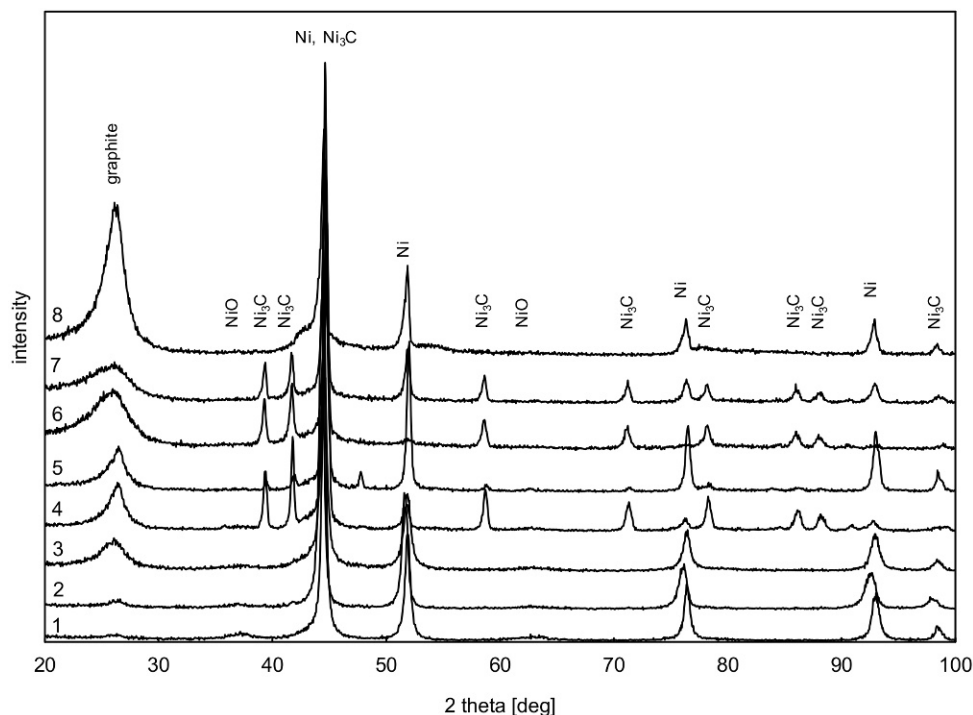
Fig. 2. Diffraction patterns of nickel catalyst after the decomposition of methane at 500 °C (1), 700 °C (2); ethane at 500 °C (3), 650 °C (4), 700 °C (5); and ethylene at 500 °C (6), 600 °C (7), 700 °C (8).

composition of the samples obtained using nickel catalyst. In the methane molecule, the ratio of hydrogen to carbon atoms is the higher than in the case of ethane and ethylene. The presence of hydrogen in the reaction space led to reduction of the formed nickel carbide, and thus the diffraction peaks of Ni_3C were not detected in the corresponding XRD spectra. In the case of decomposition of ethane and ethylene, smaller amounts of hydrogen were formed, thus the conditions to obtain nickel carbide were more favorable.

Both in the case of ethane and ethylene decomposition, the characteristic peaks of nickel carbide were observed. XRD results revealed that after ethane decomposition at 700 °C only a small amount of Ni_3C was present in the sample, whereas under the same conditions, but with ethylene as a carbon source, nickel carbide was no longer present. This indicates that at higher temperatures, the reaction equilibrium shifted towards Ni_3C decomposition, whereas the reaction rate of nickel carbide decomposition was higher than its formation rate.

Diffraction patterns of iron catalyst after the decomposition of methane at 500 °C (1), 600 °C (2), 700 °C (3); ethane at 500 °C (4), 700 °C (5); and ethylene at 500 °C (6), 600 °C (7), 700 °C (8) are shown in Fig. 3. Regardless of the carbon source and the temperature, the characteristic peaks of iron, cementite and graphite were detected in all samples. A small amount of iron oxide was also observed, especially at 500 °C. Regardless of the kind of hydrocarbons, more intense Fe_2O_3 peaks were detected at lower temperatures. Simultaneously, the ratio of carbon to iron was lower and only a low-intensity graphite peak was observed. Presumably, at lower temperatures, iron crystallites were not sufficiently covered with carbon and a part of the surface was exposed to oxidation in air.

In the samples obtained using methane, ethane and ethylene, the intensity of the iron peaks was higher when the temperature increased, while the intensity of the cementite peaks decreased at the same temperature. This phenomenon can be explained as follows. At higher temperature, more carbon was
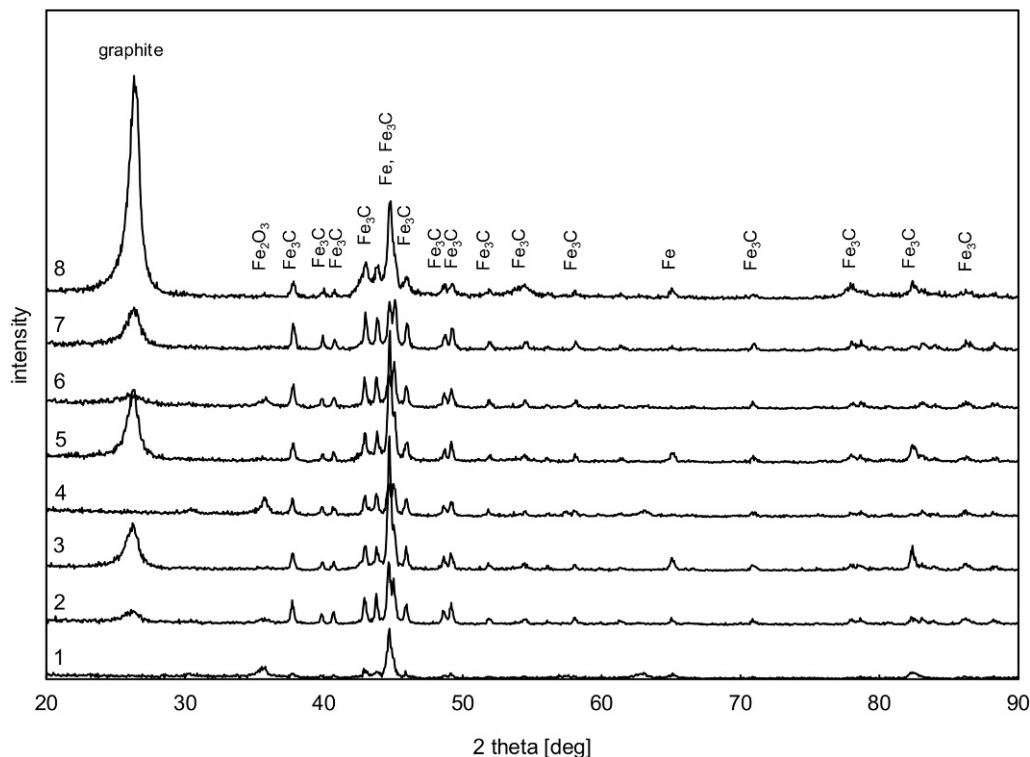
Fig. 3. Diffraction patterns of iron catalyst after the decomposition of methane at 500 °C (1), 600 °C (2), 700 °C (3); ethane at 500 °C (4), 700 °C (5); ethylene at 500 °C (6), 600 °C (7), 700 °C (8).

formed and the iron surface, necessary for hydrocarbon adsorption and decomposition, was blocked. This phenomenon prevented complete conversion of iron into cementite. Another explanation was given by Buyanov *et al.* [10, 11], who studied the formation of cementite and concluded that Fe_3C decomposes at temperatures higher than 500 °C. Therefore, the iron concentration in the samples should be higher at higher temperatures.

In order to determine how the contribution of iron and cementite in the samples changed with temperature, the intensities of the individual peaks of iron (200) and cementite (112) were taken into account to determine the Fe_3C/Fe ratio in the samples after ethane and ethylene decomposition. Subsequently, the diffraction patterns of these peaks were collected more precisely in the narrow angle range and the intensities (expressed as peak surface areas) of the individual peaks were taken into consideration. The dependence of the Fe_3C/Fe peak intensity ratio on temperature is presented in Fig. 4. Despite

significant difference in carburisation degree of the sample after ethylene and ethane decomposition, the intensity ratios of cementite to iron were very similar. Therefore, the iron concentration in the samples after hydrocarbon decomposition was independent of the amount of carbon. These observations confirm that the higher iron amounts in the samples obtained at higher temperatures were not due to unconverted iron, but to the decomposition of cementite, supporting the concept of the "carbide cycle" mechanism described by Buyanov *et al.* [10, 11].

4. Conclusions

The studies of the decomposition of methane, ethane and ethylene on iron and nickel catalysts confirmed that the formation of nanocarbons (CNTs, CNFs) occurs through the decomposition of the corresponding metal carbides, in accordance with the previous observation that nanocarbons can be formed preferentially on metals able to form un-
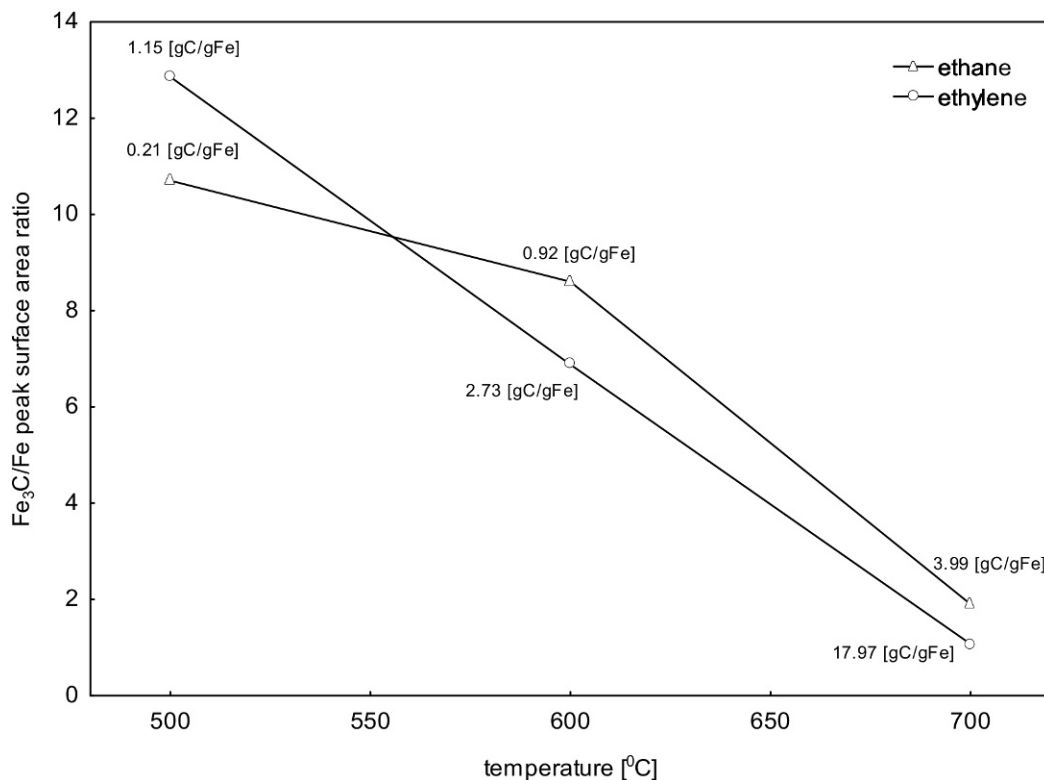
Fig. 4. The Fe₃C/Fe peak intensity ratio as a function of temperature.

stable carbides. The results of our studies confirm the existence of the "carbide cycle" proposed by Buyanov *et al.* [10, 11]. According to our studies, the Fe/Fe₃C ratio does not depend on the degree of carburisation, nor on the kind of hydrocarbon (C_2H_6 or C_2H_4), but increases with temperature.

The proposed mechanism is important for the formation and yield of nanocarbons – carbon nanotubes, nanohorns and nanocapsules.

References

[1] MARTIN-GULLON I., VERA J., CONESA J.A., GONZÁLEZ J.L., MERINO C., *Carbon*, 44 (2006) 1572.

[2] ROMERO A., GARRIDO A., NIETO-MÁRQUEZ A., SÁNCHEZ P., DE LUCAS A., VALVERDE J.L., *Micro. Meso. Mater.*, 110 (2008), 318.

[3] TRAN K.Y., HEINRICHS B., COLOMER J-F., PIRARD J-P., LAMBERT S., *Appl. Catal. A: General*, 318 (2007), 63.

[4] LEE C.J., PARK J., YU J.A., *Chem. Phys. Lett.*, 360 (2002), 250.

[5] VENEGONI D., SERP P., FEURER R., KIHN Y., VAHLAS C., KALCK P., *Carbon*, 40 (2002), 1799.

[6] PARK C,. KEANE M.A., *J. Catal.*, 221 (2004), 386.

[7] LOUIS B. *et al.*, *Catal. Today*, 102–103 (2005), 23.

[8] DECK C.P, VECCHIO K., *Carbon*, 44 (2006), 267.

[9] CH. EMMENEGGER *et al.*, *Carbon*, 41 (2003), 539.

[10] CHESNOKOV V.V., BUYANOV R.A., *Kinet. Katal.*, 28 (1987), 403.

[11] CHESNOKOV V.V., BUYANOV R.A., *Russ. Chem. Rev.*, 69 (2000), 623.

[12] ZAIKOVSKII V.I., CHESNOKOV V.V., BUYANOV R.A., *Kinet. Catal.*, 42 (2001), 813.

[13] ERMAKOVA M.A., ERMAKOV D. YU, CHUVILIN A.L., KUVSHINOV G.G., *J. Catal.*, 201 (2001), 183.

[14] BOKHONOV B., KORCHAGIN M., *J. Alloys Comp.*, 333 (2002), 308.

[15] HERNADI K., FONSECA A., NAGY J.B., BERNAERTS D., LUCAS A.A., *Carbon*, 34 (1996), 1249.

[16] HERNADI K., FONSECA A., NAGY J.B., FUDALA A., BERNAERTS D., KIRICSI I., *Appl. Catal. A: General*, 228 (2002), 103.

[17] LOUIS B. *et al.*, *Catal. Today*, 102–103 (2005), 23.

[18] GULINO G. *et al.*, *Appl. Catal. A: General*, 279 (2005), 89–97.

[19] TAKENAKA S., SERIZAWA M., OTSUKA K., *J. Catal.*, 222 (2004), 520.